Nanoscale

RSC Publishing

PAPER

View Article Online
View Journal

Cite this: DOI: 10.1039/c3nr01598j

A functional glycoprotein competitive recognition and signal amplification strategy for carbohydrate–protein interaction profiling and cell surface carbohydrate expression evaluation†

Yangzhong Wang, Zhuhai Chen, Yang Liu* and Jinghong Li

A simple and sensitive carbohydrate biosensor has been suggested as a potential tool for accurate analysis of cell surface carbohydrate expression as well as carbohydrate-based therapeutics for a variety of diseases and infections. In this work, a sensitive biosensor for carbohydrate–lectin profiling and *in situ* cell surface carbohydrate expression was designed by taking advantage of a functional glycoprotein of glucose oxidase acting as both a multivalent recognition unit and a signal amplification probe. Combining the gold nanoparticle catalyzed luminol electrogenerated chemiluminescence and nanocarrier for active biomolecules, the number of cell surface carbohydrate groups could be conveniently read out. The apparent dissociation constant between GOx@Au probes and Con A was detected to be 1.64 nM and was approximately 5 orders of magnitude smaller than that of mannose and Con A, which would arise from the multivalent effect between the probe and Con A. Both glycoproteins and gold nanoparticles contribute to the high affinity between carbohydrates and lectin. The as-proposed biosensor exhibits excellent analytical performance towards the cytosensing of K562 cells with a detection limit of 18 cells, and the mannose moieties on a single K562 cell were determined to be 1.8×10^{10}. The biosensor can also act as a useful tool for antibacterial drug screening and mechanism investigation. This strategy integrates the excellent biocompatibility and multivalent recognition of glycoproteins as well as the significant enzymatic catalysis and gold nanoparticle signal amplification, and avoids the cell pretreatment and labelling process. This would contribute to the glycomic analysis and the understanding of complex native glycan-related biological processes.

Received 31st March 2013
Accepted 3rd June 2013

DOI: 10.1039/c3nr01598j

www.rsc.org/nanoscale

1 Introduction

Carbohydrates have intrigued scientists for decades as mediators of a myriad of biological events. With respect to the structural diversity, carbohydrates encode much information for specific molecular recognition and serve as determinants of protein folding, trafficking and stability, and pharmacokinetics.[1,2] Abnormal expression of carbohydrates on cell surfaces has been shown to be associated with many diseases, such as cancer and Alzheimer's disease.[3–6] The interaction of carbohydrate and carbohydrate-binding proteins, so-called lectin, plays significant roles in diverse processes such as bacterial or viral infection, cell communication, inflammation, immune response modulation, cell growth and development, and signal transduction.[7–10] The analysis of carbohydrate–protein interactions (structure and thermodynamic and kinetic parameters) is of fundamental importance and facilitates the design of carbohydrate-based therapeutics for a variety of diseases and infections.[11] Various methods such as isothermal titration calorimetry assay, surface plasmon resonance, fluorescence polarization, field effect transistors, quartz crystal microbalance and electrochemical impedance spectroscopy have been employed towards probing carbohydrate–lectin interactions and cell surface carbohydrates.[6,12–19] However, the less active accessibility and weak affinity between monosaccharides and lectin as well as the loss of biocompatibility during the electrode modification still limit the sensitivity and stability of these methods. Understanding and mimicking specific interactions and functions between native carbohydrates and proteins in the biological processes is highly desirable for clinical diagnostics and therapeutics.

Glycoproteins consist of proteins covalently linked to carbohydrates, and fifty percent of all proteins are known to be glycosylated. The majority of biomacromolecules such as enzymes, antibodies, hormones, *etc.* are glycoproteins. Besides

Department of Chemistry, Beijing Key Laboratory for Microanalytical Methods and Instrumentation, Key Laboratory of Bioorganic Phosphorus Chemistry & Chemical Biology, Tsinghua University, Beijing 100084, China. E-mail: liu-yang@mail.tsinghua.edu.cn; Fax: +86-10-62771149; Tel: +86-10-62795290

† Electronic supplementary information (ESI) available: Experimental details; characterization of probes; the influence of electrolyte pH; probe concentration and glucose concentration on the electrode ECL effect. See DOI: 10.1039/c3nr01598j

the importance in biological recognition, carbohydrates contribute to the specific structure and diverse function of various glycoproteins that ensure the effective modulation of cell signalling and metabolism.[1,2,5,8,9,20] Introduction of competitive recognition of glycoproteins will not only bring about the native multivalent carbohydrate–protein interaction but also afford biocompatible amplification probes for signal transduction that improves the sensitivity and stability of a carbohydrate biosensor.

Owing to their good biocompatibility, fascinating electrocatalytic activity, large surface area, and excellent photo- and electronic features, nanostructure materials such as gold nanoparticles, quantum dots, carbon nanotubes, *etc.* have received much attention in electrochemistry, biosensing and imaging and so on.[21–24] Moreover, the unique properties of nanomaterials allow them to be interfaced with biomolecules such as nucleic acids, proteins, peptides and so on, and open up a wide range of biological applications. Nanomaterials can also function as efficient scaffolds for multiple carbohydrate presentation to achieve sufficiently high affinities required for sensitive recognition.[14,18,25]

Electrogenerated chemiluminescense (ECL) is a light emission that arises from the high-energy electron-transfer reaction between electrogenerated species at electrode surfaces. This technique shows potential- and spatial-controlled properties, and is highly sensitive. By integrating the interactions between biomolecules, the ECL assay has become a powerful analytical tool for highly sensitive and specific detection in biochemistry, and is widely used in immunoassays, DNA analysis, environmental detection and clinical diagnostics.[26–29]

In this work, a sensitive ECL method was developed to study carbohydrate–protein interactions and cell surface carbohydrate expression evaluation by integrating the competitive recognition and biocatalysis of glycoproteins as well as the excellent electrocatalytic activity of gold nanoparticles for luminol ECL reactions, and glucose oxidase was used as a model glycoprotein which is an important mannose-containing glycoprotein that catalyses the oxidation of glucose to D-glucono-δ-lactone and aids in breaking the sugar down into its metabolites in cells.[30] The carbohydrate–protein interactions between Con A and mannose, mannan and GOx conjugated gold nanoparticles were investigated. Moreover, the as-proposed ECL method was also used for cell detection as well as cell surface carbohydrate expression evaluation. Such a simple and sensitive carbohydrate biosensor would be promising in reliable diagnostics of glycan relevant biomarkers for cancer and other diseases.

2 Experimental section

Materials and reagents

Bovine serum albumin (BSA) was purchased from Dingguo Biological Products Company (China). Glucose oxidase (GOx, 100–250 units per mg) was obtained from Sangon Biotech (China). Luminol and mannan (average molar mass is about 48 kDa) were received from Sigma-Aldrich (USA). $HAuCl_4 \cdot 3H_2O$ (48% w/w) was obtained from Shanghai Reagent (China). D-Mannose was provided by Alfa Aesar (USA). Other reagents of analytical grade were obtained from Sinopharm Chemical Reagent Company (China) and were used as received. Phosphate buffer solutions (PBS) were prepared with $Na_2HPO_4 \cdot 12H_2O$ and $NaH_2PO_4 \cdot 2H_2O$, containing 137 mM NaCl and 2.7 mM KCl.

Cell line, culture and treatment

The K562 cell line was kindly provided by the medical college of Tsinghua University. K562 cells were cultured in RPMI 1640 medium (Dingguo) supplemented with fetal bovine serum (10%, Dingguo), penicillin (100 U mL^{-1}), and streptomycin (100 U mL^{-1}) at 37 °C in a humid atmosphere containing CO_2 (5%). The cells in exponential growth phase were collected and separated by centrifugation at 800 rpm for 5 min. The cell number was determined using a blood counting chamber.

Preparation of glucose oxidase (GOx) conjugated gold nanoprobes

The gold nanoparticles were prepared as reported previously.[31] In brief, 2.5 mL of 4 g mL^{-1} $HAuCl_4$ solution and 97.5 mL deionized water were added into a round flask and heated to boiling. Then, 5 mL of 10 mg mL^{-1} sodium citrate solution was added rapidly under vigorous stirring. The solution was maintained at the boiling state for 15 min until the colour changed from yellow to deep wine red, and the gold particles formed. The GOx conjugated gold nanoparticles were prepared by adding 3 mg GOx to 3 mL of gold colloidal solution and gently stirred for 10 h. Then, the mixture was centrifuged at 10 000 rpm for 10 min and washed with deionized water. Finally, the sediment was resuspended in 1.5 mL PBS (pH 7.4) containing 0.48 mM Ca^{2+} and 0.48 mM Mn^{2+}. The resulting gold nanoparticles were characterized by transmission electron microscopy (TEM) and UV-vis spectroscopy. Statistical analysis of TEM data revealed that the average diameter of the gold nanoparticles was about 20 nm. The as-prepared GOx@Au nanoprobes were characterized by TEM and UV-vis (Fig. S1 in the ESI†). The size of the probes was about 20 nm from the TEM image. From the UV-vis absorption spectrum, also the concentration of Au nanoparticles was estimated to be 1.87 nM.[2] After the conjugation of GOx, the characteristic absorption peak of gold nanoparticles red shifts from 520 nm to 525 nm due to the decoration of GOx on Au nanoparticles.

Fabrication of the Con A modified electrode

A gold electrode (diameter of 2 mm) was polished carefully first with 0.3 μm α-Al_2O_3 powder, and washed ultrasonically with ethanol and water. Prior to immobilization of Con A, the gold electrode was scanned in 0.5 M H_2SO_4 between 0.2 and 1.65 V (*vs.* Ag/AgCl) until a reproducible cyclic voltammogram curve was obtained. After drying with N_2, the gold electrode was immersed in a 100 μL PBS (0.01 M, pH 7.4) solution containing 2 mg mL^{-1} Con A for 14 h. The resulting electrode was rinsed thoroughly with PBS, followed by immersing in 2 mg mL^{-1} BSA for 1 h to block the nonspecific binding sites on the electrode. The electrode was then carefully rinsed with PBS to remove the

excess BSA. To determine the target cells and carbohydrates, the Con A modified electrode was immersed in glucose oxidase conjugated gold colloidal solution for 1 h, and washed with deionized water. After that, target cells and carbohydrates were detected by dipping the electrode in a solution containing a certain concentration of target samples and incubating for 2 h. The obtained electrode was then rinsed with deionized water and was characterized in a luminol solution. In the experiments for the interaction between Con A and mannose or mannan, the Con A/Au electrode was immersed in a 100 μL PBS solution containing 0.48 mM Ca^{2+}, 0.48 mM Mn^{2+}, 3.4 nM GOx@Au nanoparticles and mannose (or mannan) at a certain concentration for 2 h. Then the electrode was washed with PBS and subjected to the ECL characterization.

Apparatus

Transmission electron microscope (TEM) images were obtained with a JEM-2010 high-resolution TEM system (JEOL, Japan). The UV-vis experiment was performed with a UV-3900 spectrophotometer (Hitachi, Japan). The cyclic voltammetry was conducted on a CHI 660b instrument (CH Instrument Co.). Electrochemical impedance spectroscopy (EIS) was carried out on a PARSTAT 2273 potentiostat/galvanostat (Advanced Measurement Technology Inc.) by applying an ac voltage of 5 mV amplitude in the 0.01 Hz to 10^5 Hz frequency range in a solution containing 5 mM $K_3[Fe(CN)_6]/K_4[Fe(CN)_6]$ and 0.1 M KCl. The ECL measurements were carried out on an MPI-B multifunctional electrochemical analytical system (Xi'an Remex Analytical Instrument Ltd. Co., China). If no special statement was made, the ECL measurements were performed in a 0.1 M PBS (pH 7.86) containing 100 μM luminol and 0.1 M glucose at a scan rate of 100 mV s^{-1} and the voltage of PMT was maintained at 600 V.

3 Results and discussion

Scheme 1 displays the configuration of the biosensor for carbohydrate–protein interaction and tumor cell detection. A mannose recognized lectin, Concanavalin A (Con A), was first immobilized on a gold electrode, and bovine serum albumin (BSA) was used as a blocking layer to avoid nonspecific adsorption. Due to the large surface area and excellent catalytic properties of gold nanoparticles, a multifunctional probe of GOx coupled gold nanoparticles was fabricated as the recognition and amplification probe. Besides the specific interaction between the mannoses in GOx molecules and Con A that forms a supermolecular complex structure on the electrode, GOx also catalyses the oxidation of glucose to produce hydrogen peroxide which significantly improves the ECL signal of luminol. Moreover, the introduction of gold nanoparticles by immobilizing GOx on the surface of gold nanoparticles (GOx@Au) can further improve the ECL signal due to the excellent catalytic activity of gold nanoparticles toward luminol ECL reaction and their large surface area that can accommodate a large number of GOx molecules on the surface.[32] In the presence of mannose or mannose-containing glycoproteins, the probes compete with the mannose sites, and thus decrease the ECL signal, which can be applied in carbohydrate–protein interaction profiling and carbohydrate expression evaluation.

Cyclic voltammetry (CV) was employed to evaluate the assembly processes by monitoring the electron transfer ability tunneling through the barrier layer between the electroactive probes and the gold electrode. Fig. 1A shows the CV curves presenting the step-by-step build up process on the gold electrode using $Fe(CN)_6^{4-/3-}$ as electroactive probes. As can be seen, a couple of quasi-reversible redox peaks were obtained for the bare gold electrode (curve a). When the gold electrode was treated with Con A, the layer of Con A on the gold electrode led

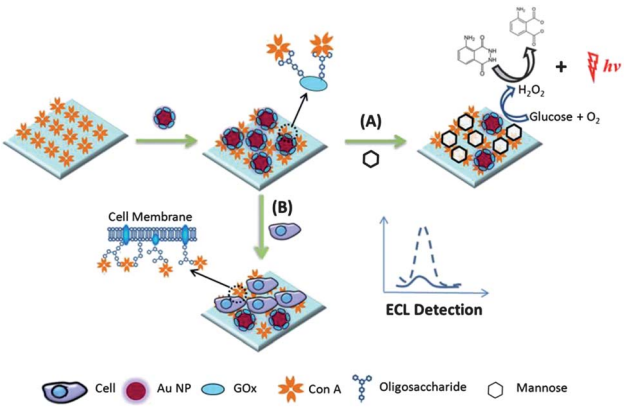

Scheme 1 Configurations of the functional glycoprotein competitive recognition ECL strategy for carbohydrate–protein interaction analysis (A) and cell surface carbohydrate expression (B).

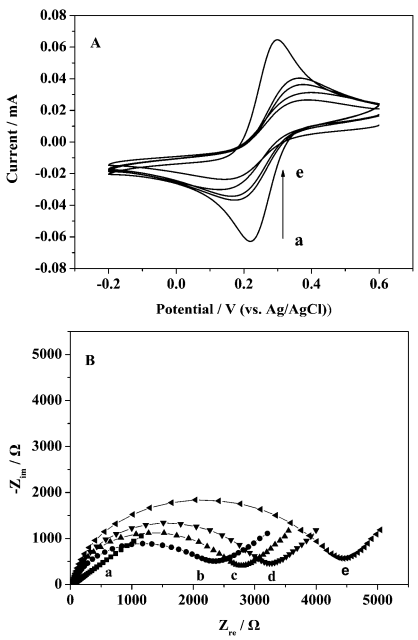

Fig. 1 Cyclic voltammograms (A) and electrochemical impedance spectra (B) of bare GE (a), Con A/GE (b), BSA/Con A/GE (c), GOx@Au/BSA/Con A/GE (d), and GOx@Au/cells/BSA/Con A/GE (e). These experiments were conducted in 0.1 M KCl solution with 5 mM $[Fe(CN)_6]^{3-/4-}$ electroactive probes. Scan rate is 100 mV s^{-1}. The frequency range is between 0.01 Hz and 10^5 Hz with a signal amplitude of 5 mV in panel B.

to a decrease of peak current (curve b), ascribed to the electronically inert feature of Con A that partially blocks the electron transfer and mass transfer of $Fe(CN)_6^{4-/3-}$ couple ions at the electrode interface. After the modification of the BSA blocking layer, the peak current in the CV decreased further and the potential gap between the anodic and cathodic peaks became wider (curve c). When GOx@Au probes were added, it was found that the peak current also decreased. The decreased current should be resulted from the inert GOx molecules which formed an inert coating on gold nanoparticles and inhibited the electron transfer even though gold nanoparticles had good conductivity. In addition, the negatively charged GOx coating of GOx@Au probes may also block the mass transfer of $Fe(CN)_6^{4-/3-}$ probes due to the electrostatic repulsion interaction. When the electrode was immersed in the solution containing K562 cells, the peak current decreased further due to the replacement of GOx@Au probes by K562 cells. It is reasoned that the K562 cells are totally electronically inert, and the size of the cells is large, which would not only decrease the electron transfer ability but also inhibit the mass transfer of $Fe(CN)_6^{4-/3-}$ probes toward the modified electrode. These phenomena were also confirmed by the electrochemical impedance spectra (EIS) as shown in Fig. 1B. In the Nyquist plot, the diameter of the semi-circle in a higher frequency range is equal to the electron transfer resistance, which represents the electron transfer kinetics of the electroactive probes at the electrode interface. It was clear that the diameter of the semi-circle after the assembly of Con A (curve b) and BSA (curve c) was larger than that of a bare gold electrode (curve a), indicating an increase of the electron transfer resistance after the assembly of Con A and BSA on the gold electrode. The electron transfer resistance increased further after the assembly of GOx@Au probes (curve d) and the competing adsorption of K562 cells (curve e). The phenomena are consistent with those in the CV. The facts elucidate that the gold electrodes are step-by-step assembled by Con A, BSA, GOx@Au probes and K562 cells.

Fig. 2A presents the ECL responses of a Con A modified electrode (curve a) and GOx@Au assembled on a Con A modified electrode (curve e) blocking by BSA in the solution containing luminol and glucose. The peaks at *ca.* 0.58 V in curves result from the ECL reaction of luminol. The bare gold electrode presents a quite weak signal, and the ECL signal decreases after the modification of Con A and BSA due to the electron transfer inhibition on the electrode interface by the electron inert biomolecules (curve c in Fig. S2, ESI†). After incubating the BSA/Con A/GE in GOx@Au colloidal solution, the modified electrode gives a strong ECL signal (curve e). What is more, the ECL signal of the bare gold electrode with treatment of GOx@Au was weak but higher than that of the bare gold electrode without GOx@Au treatment (curve d in Fig. S2, ESI†), which could arise from the nonspecific adsorption of GOx@Au by electrostatic interactions.[33] However, if the bare gold electrode was blocked by BSA only, the nonspecific adsorption could be avoided effectively. In addition, the ECL intensity was also weak by incubating the BSA/Con A/GE in bare gold nanoparticle colloidal solution, but it was larger than that without incubation (curve b in Fig. S2, ESI†), which could be ascribed to the

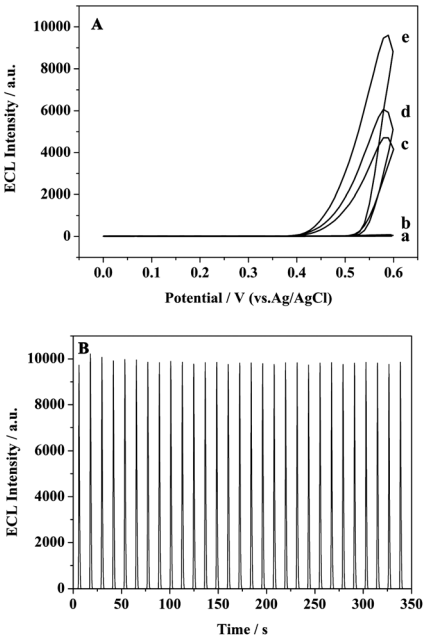

Fig. 2 (A) ECL–potential curves of BSA/Con A/GE (a), GOx@Au/BSA/Con A/GE (b and e), GOx/BSA/Con A/GE (d) and mannose competed GOx@Au/BSA/Con A/GE (c) in a 0.1 M PBS (pH 7.86) solution containing 100 μM luminol with (a, c, d, and e) and without (b) 0.1 M glucose. The concentrations of GOx and mannose were 1.4×10^{-3} mg mL^{-1} and 0.09 mg mL^{-1} respectively. (B) ECL–time curve of the GOx@Au/BSA/Con A/gold electrode in a 0.1 M PBS (pH 7.86) solution containing 100 μM luminol and 0.1 M glucose. Scan rate, 100 mV s^{-1}. The voltage of PMT was maintained at 600 V.

nonspecific adsorption of Au nanoparticles that facilitated the electron transfer at the electrode interface and catalysed the ECL process of luminol.[34] These results confirmed that the strong ECL signal was ascribed to the specific recognition between mannose in GOx and Con A. The ECL behaviour of GOx@Au/BSA/Con A/GE was also studied in luminol solution with and without glucose. The ECL signal decreased quickly (curve b) when the GOx@Au/BSA/Con A/GE was characterized in luminol solution without glucose. This signified that the intense ECL signal originated from the GOx mediated electrooxidation of glucose that produced the H_2O_2 and improved the ECL reaction of luminol. When only GOx was adsorbed to the BSA/Con A/GE, the ECL intensity was also strong (curve d), but it was weaker than that of GOx@Au/BSA/Con A/GE. This result verifies that both enzymatic amplification and gold nanoparticle catalysis lead to the strong ECL signal of luminol. The ECL signal of the GOx@Au modified BSA/Con A/GE was sensitive to mannose and mannose containing glycoproteins, and it decreased by dipping the modified electrode into the incubating solution containing mannose (curve c) because of the competing reaction between GOx@Au and mannose on the electrode surface. Specifically, the ECL emission based on the supermolecular assembly strategy was very stable. No obvious change was observed (Fig. 1B) upon successive scans. The result suggests that the designed interface is suitable for ECL detection. Such a multifunctional carbohydrate recognition and catalytic amplification will be useful to understand the

complicated biological recognition and metabolism processes and develop novel biosensors with high performances.

In the ECL assay, the GOx@Au probes competed with the mannose or mannose-containing glycoprotein, and two equilibriums, mannose with Con A and GOx@Au with Con A, were established in this process. This competitive recognition changed the ECL signal so that the affinity between the mannose containing glycoprotein and Con A can be analysed. Fig. 3 shows the ECL response in the presence of mannose (A) and mannan (B) at different concentrations. From the concentration–ECL response curve (Fig. 3A), their IC_{50} values and the apparent dissociation constant (K_D) can be obtained according to the Cheng–Prusoff equation.[18] The K_D between mannose and Con A was calculated to be 1.34×10^{-4} M by the ECL assay, which is comparable to a previously published value (2.00×10^{-4} M) by SPR.[35] In nature, multivalent interactions between the binding proteins and the carbohydrate ligands are always important that significantly enhance their affinity. To further understand the interaction between carbohydrate and lectin, we analysed the binding affinity between Con A and mannan which is a mannose polymer, and its K_D value was calculated to be 1.59×10^{-8} M which was similar to those previously reported by the methods of isothermal sorption (5.20×10^{-8} M) and spectral phase interference (3.33×10^{-8} M),[36,37] and was approximately 4 orders of magnitude smaller than that of mannose and Con A. In addition, the apparent dissociation constant between Con A and GOx was also calculated to be 4×10^{-7} M. This result was similar to those reported earlier, but three orders of magnitude larger than that of mannose and Con A.[38] However, it was two orders of magnitude larger than that of GOx@Au (1.64 nM) and Con A (Fig. S3B in the ESI†). These results demonstrated that both GOx and gold nanoparticles contribute to the high affinity of Con A and carbohydrate probes, which would arise from the multivalent effect between the probe and Con A.[11,39] Such a probe with high affinity and biocompatibility would be promising as a sensitive biosensor for clinical diagnostic application.

As illustrated in Scheme 1, the ECL biosensor can be used for effective tumor cell analysis based on the specific interactions between lectin and carbohydrates on cell surfaces.[25] Fig. 4A presents the ECL response of the biosensor to tumor cells using K562 cells as a model. Upon increasing the concentration of K562 cells, the ECL intensity decreased due to the competition between the cells and GOx@Au probes. The ECL intensity decreased linearly with the cell concentration over the range from 4.2×10^3 to 3.0×10^6 cells per mL (Fig. 4B). The limit of detection was 1.8×10^3 cell per mL at 3σ. Taking into account that 10 μL of K562 cell suspension was used for incubation, the ECL strategy achieved the limit of detection of only 18 K562 cells. Assuming that the cell had the same binding kinetics with the mannose containing glycoproteins, the cell surface mannose quantities could be equal to the active mannose amount entirely replacing the probes on the electrode. In this way, the mannose moieties on the K562 cell surface were estimated to be 1.8×10^{10}, which was similar to that obtained by electrochemical and enzymatic methods.[19,40] These results demonstrate that the proposed ECL strategy is suitable for sensitive cell surface carbohydrate expression evaluation. Such a simple and sensitive biosensor is promising in the applications of *in situ* carbohydrate expression and tumor cell determination.

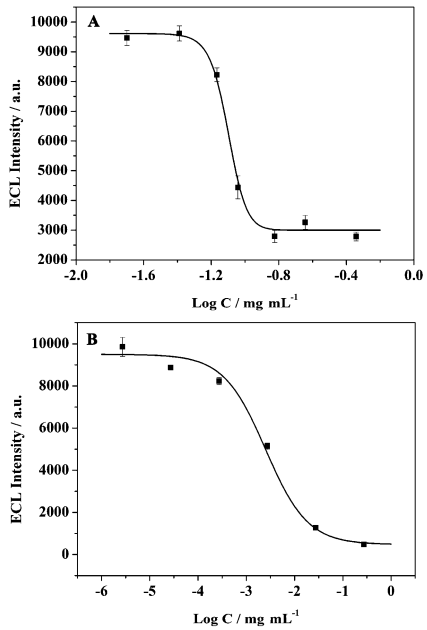

Fig. 3 The ECL intensity as a function of the concentration logarithm of mannose (A) and mannan (B).

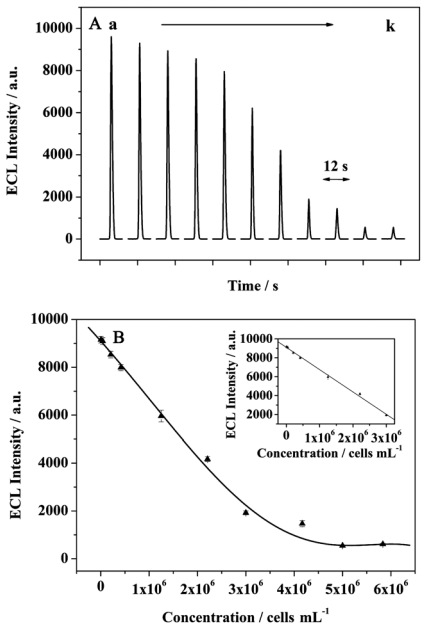

Fig. 4 (A) ECL–time behaviours of GOx@Au/BSA/Con A/GE at different concentrations of K562 cells: (a) 0, (b) 4.2×10^3, (c) 4.2×10^4, (d) 2.1×10^5, (e) 4.2×10^5, (f) 1.3×10^6, (g) 2.2×10^6, (h) 3.0×10^6, (i) 4.2×10^6, (j) 5.0×10^6, (k) 5.8×10^6 cells per mL. (B) ECL intensity as a function of the concentration of K562 cells. The inset shows the linear relationship between the ECL intensity and the K562 cell concentration.

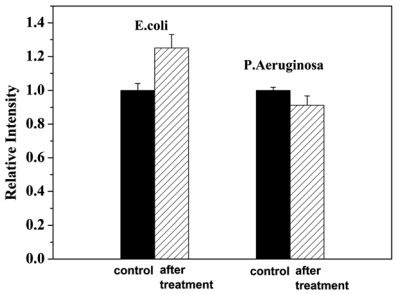

Fig. 5 The relative intensity of *P. aeruginosa* ATCC27853 and *E. coli* ATCC11775 before (control) and after gentamicin treatment (after treatment) respectively. The bacteria concentration is 5×10^6 cells per mL. The ECL measurements were performed in a 0.1 M PBS (pH 7.86) solution containing 100 μM luminol and 0.1 M glucose at a scan rate of 100 mV s^{-1}. The voltage of PMT was maintained at 600 V.

Carbohydrates on a bacterial surface play an important role in bacterial infection. The main bacterial cell wall component in all Gram-negative bacteria families consists of a class of glycoconjugates called lipopolysaccharides (LPS) which occupies about 75% of bacterial surface area.[41] LPS of Gram-negative bacteria is the most striking character for bacteria and provides the selective specificity needed for lectin recognition, which could not only be applied to the bacterial detection but also antibacterial drug screening and interaction mechanism studies. Gentamicin is an aminoglycoside antibiotic, used to treat many types of bacterial infections particularly Gram-negative organisms, which can destroy the cell membrane and may also affect the expression of LPS on the bacterial surface.[42] Fig. 5 shows the relative ECL intensity of *P. aeruginosa* ATCC27853 and *E. coli* ATCC11775 before and after gentamicin treatment respectively. It was obvious that different carbohydrate expression behaviors between *P. aeruginosa* and *E. coli* were presented after gentamicin treatment. The increased ECL intensity means that the expression of LPS on the *E. coli* was inhibited after gentamicin treatment. However, when the *P. aeruginosa* was treated with gentamicin, the ECL intensity increased, which means that the LPS expression decreased. It is known that *P. aeruginosa* shows some resistance to gentamicin which may cause the expression of some carbohydrates such as alginate on its surface, which can also bind with Con A.[43] These results demonstrate that the biosensor can be promising in the applications of antibiotic interaction mechanism studies on bacterial infection.

4 Conclusion

In conclusion, a sensitive ECL biosensor for carbohydrate–lectin profiling and *in situ* cell surface carbohydrate expression evaluation was designed by taking advantage of a functional glycoprotein acting as both a multivalent recognition unit and a signal amplification probe. This biosensor integrates the excellent biocompatibility and multivalent recognition of glycoproteins as well as the significant enzymatic catalysis and gold nanoparticle signal amplification, and possesses high sensitivity, perfect stability and reproducibility for cell detection and cell surface carbohydrate expression evaluation. Such a carbohydrate biosensor also acts as a useful tool for antibacterial drug screening and interaction mechanism studies. This glycoprotein recognition and biocatalysis biosensing strategy would contribute to the understanding of complex native glycan-related biological processes.

Acknowledgements

This work was financially supported by the National Basic Research Program of China (no. 2011CB935704), the National Natural Science Foundation of China (no. 21235004, no. 21128005, no. 21005046), the European Union Seventh Framework Programme (FP7/2007–2013) under grant agreement no. 260600 ("GlycoHIT") and the Specialized Research Fund for the Doctoral Program of Higher Education (no. 20100002120042).

Notes and references

1 C. R. Bertozzi and L. L. Kiessling, *Science*, 2001, **291**, 2357–2364.
2 J. Finkelstein, *Nature*, 2007, **446**, 999.
3 J. E. Rexach, P. M. Clark and L. C. Hsieh-Wilson, *Nat. Chem. Biol.*, 2008, **4**, 97–106.
4 S. A. Yuzwa, X. Shan, M. S. Macauley, T. Clark, Y. Skorobogatko, K. Vosseller and D. J. Vocadlo, *Nat. Chem. Biol.*, 2012, **8**, 393–399.
5 D. H. Dube and C. R. Bertozzi, *Nat. Rev. Drug Discovery*, 2005, **4**, 477–488.
6 W.-W. Zhao, L. Zhang, J.-J. Xu and H.-Y. Chen, *Chem. Commun.*, 2012, **48**, 9456–9458.
7 C. M. Szymanski and B. W. Wren, *Nat. Rev. Microbiol.*, 2005, **3**, 225–237.
8 M. D. Mager, V. LaPointe and M. M. Stevens, *Nat. Chem.*, 2011, **3**, 582–589.
9 C.-Y. Wu and C.-H. Wong, *Chem. Commun.*, 2011, **47**, 6201–6207.
10 Y. Wang, S. Chalagalla, T. Li, X.-l. Sun, W. Zhao, P. G. Wang and X. Zeng, *Biosens. Bioelectron.*, 2010, **26**, 996–1001.
11 Y. Sato, K. Yoshioka, T. Murakami, S. Yoshimoto and O. Niwa, *Langmuir*, 2012, **28**, 1846–1851.
12 G. Bellapadrona, A. B. Tesler, D. Gruenstein, L. H. Hossain, R. Kikkeri, P. H. Seeberger, A. Vaskevich and I. Rubinstein, *Anal. Chem.*, 2012, **84**, 232–240.
13 K. Kakehi, Y. Oda and M. Kinoshita, *Anal. Biochem.*, 2001, **297**, 111–116.
14 H. Vedala, Y. Chen, S. Cecioni, A. Imberty, S. Vidal and A. Star, *Nano Lett.*, 2011, **11**, 170–175.
15 J. T. La Belle, J. Q. Gerlach, S. Svarovsky and L. Joshi, *Anal. Chem.*, 2007, **79**, 6959–6964.
16 Z. Shen, M. Huang, C. Xiao, Y. Zhang, X. Zeng and P. G. Wang, *Anal. Chem.*, 2007, **79**, 2312–2319.
17 L. Ding, Q. Ji, R. Qian, W. Cheng and H. Ju, *Anal. Chem.*, 2010, **82**, 1292–1298.
18 X. Wang, O. Ramstrom and M. Yan, *Anal. Chem.*, 2010, **82**, 9082–9089.
19 L. Ding, W. Cheng, X. Wang, S. Ding and H. Ju, *J. Am. Chem. Soc.*, 2008, **130**, 7224–7225.

20 R. Jelinek and S. Kolusheva, *Chem. Rev.*, 2004, **104**, 5987–6015.
21 L. Sun, D. Liu and Z. Wang, *Anal. Chem.*, 2006, **79**, 773–777.
22 Z.-F. Zhang, H. Cui, C.-Z. Lai and L.-J. Liu, *Anal. Chem.*, 2005, **77**, 3324–3329.
23 P. Bertoncello and R. J. Forster, *Biosens. Bioelectron.*, 2009, **24**, 3191–3200.
24 J. Lei and H. Ju, *Chem. Soc. Rev.*, 2012, **41**, 2122–2134.
25 J.-J. Zhang, F.-F. Cheng, T.-T. Zheng and J.-J. Zhu, *Anal. Chem.*, 2010, **82**, 3547–3555.
26 M. M. Richter, *Chem. Rev.*, 2004, **104**, 3003–3036.
27 Y. Wang, J. Lu, L. Tang, H. Chang and J. Li, *Anal. Chem.*, 2009, **81**, 9710–9715.
28 H. Dai, Y. Y. Lin, G. F. Xu, L. S. Gong, C. P. Yang, X. L. Ma and G. N. Chen, *Electrochim. Acta*, 2012, **78**, 508–514.
29 L. Hu and G. Xu, *Chem. Soc. Rev.*, 2010, **39**, 3275–3304.
30 Z. Wen and B. Niemeyer, *J. Chromatogr., B: Anal. Technol. Biomed. Life Sci.*, 2007, **857**, 149–157.
31 K. C. Grabar, R. G. Freeman, M. B. Hommer and M. J. Natan, *Anal. Chem.*, 1995, **67**, 735–743.
32 S. Xu, Y. Liu, T. Wang and J. Li, *Anal. Chem.*, 2011, **83**, 3817–3823.
33 M. Rabe, D. Verdes and S. Seeger, *Adv. Colloid Interface Sci.*, 2011, **162**, 87–106.
34 S. Xu, Y. Liu, T. Wang and J. Li, *Anal. Chem.*, 2010, **82**, 9566–9572.
35 E. A. Smith, W. D. Thomas, L. L. Kiessling and R. M. Corn, *J. Am. Chem. Soc.*, 2003, **125**, 6140–6148.
36 D. Mislovicova, J. Masarova, J. Svitel, R. Mendichi, L. Soltes, P. Gemeiner and B. Danielsson, *Bioconjugate Chem.*, 2002, **13**, 136–142.
37 M. Hartmann, P. Nikitin and M. Keusgen, *Biosens. Bioelectron.*, 2006, **22**, 28–34.
38 J. Katrlik, R. Skrabana, D. Mislovicova and P. Gemeiner, *Colloids Surf., A*, 2011, **382**, 198–202.
39 P.-H. Liang, S.-K. Wang and C.-H. Wong, *J. Am. Chem. Soc.*, 2007, **129**, 11177–11184.
40 J. M. Francois, *Nat. Protoc.*, 2007, **1**, 2995–3000.
41 K. L. Hsu, K. T. Pilobello and L. K. Mahal, *Nat. Chem. Biol.*, 2006, **2**, 153–157.
42 D. Nelson, T. E. S. Delahooke and I. R. Poxton, *J. Med. Microbiol.*, 1993, **39**, 100–106.
43 M. Strathmann, J. Wingender and H. C. Flemming, *J. Microbiol. Methods*, 2002, 237–248.